THE JOURNAL OF PHYSICAL CHEMISTRY B

ARTICLE

pubs.acs.org/JPCB

Ligand Conformational and Solvation/Desolvation Free Energy in Protein−Ligand Complex Formation

Michal Kolář,[†] Jindřich Fanfrlík,[†] and Pavel Hobza*[,†,‡,§]

[†]Institute of Organic Chemistry and Biochemistry, Academy of Sciences of the Czech Republic and Center for Biomolecules and Complex Molecular Systems, Flemingovo nam. 2, 166 10 Prague, Czech Republic

[‡]Department of Physical Chemistry, Palacky University, 771 46 Olomouc, Czech Republic

[§]Department of Chemistry, Pohang University of Science and Technology, San 31, Hyojadong, Namgu, Pohang 790-784, Korea

Supporting Information

ABSTRACT: In this study, an extensive sampling of the conformational space of nine HIV-1 protease inhibitors was performed to estimate the uncertainty with which a single-conformation scoring scheme approximates the ligand−protein binding free energy. The SMD implicit solvation/desolvation energy and gas-phase PM6-DH2 energy were calculated for a set of 1600 conformations of each ligand. The probability density functions of the energies were compared with the values obtained from the single-conformation approach and from a short *ab initio* molecular dynamics simulation. The relative uncertainty in the score within the set of nine inhibitors was calculated to be 3.5 kcal·mol^{-1} and 2.7 kcal·mol^{-1} for the single-conformation and short dynamics, respectively. These results, though limited to the consideration of flexible ligands, provide a valuable insight into the precision of rigid models in the current computer-aided drug design.

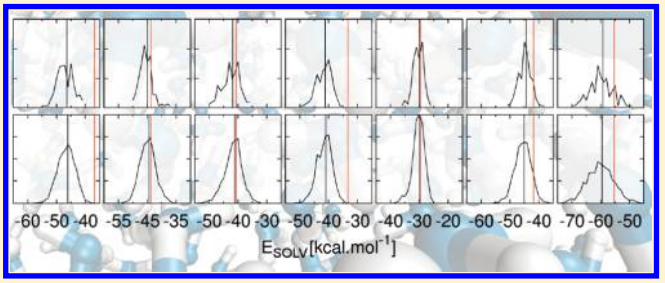

1. INTRODUCTION

Computer-assisted drug design represents an attractive and useful tool for pharmaceutical research, and the main advantage of the procedure is the expected reduction of the number of systems that should be synthesized. The modeling of the formation of the protein−ligand (P−L) complex from the free subsystems in a water environment,

$$P_w + L_w \leftrightarrow (P-L)_w \quad (1)$$

represents a crucial step in the drug-design process.[1] The aim of the theoretical description is the evaluation of the binding free energy, which is expected to be directly proportional to the ligand potency.[2] The evaluation of the absolute values of the binding free energies is impractical. The relative binding free energies for similar ligands acting on the same target can be estimated by using thermodynamic integration[3,4] or free-energy perturbation techniques.[4,5] The use of these advanced molecular dynamics methods for different ligands acting on different proteins is computationally demanding and thus limited, hence other, simpler procedures should be applied. To save computer resources, often a single-conformation approach is adopted, which means that the flexibility of the object (target, ligand or both) is neglected. Especially for high-throughput studies, the flexibility issues are beyond the limit.[6−8] Recently, we have introduced a novel protein−ligand scoring procedure based on a semiempirical quantum mechanical (SQM) Hamiltonian.[9] Here the score, which approximates the binding free energy and stands for a measure of the ligand affinity, is constructed as a sum of various contributions:[9]

1 the binding enthalpy of the P−L complex in a water environment;
2 the solvation/desolvation free energy of a ligand and protein;
3 the deformation energies of the ligand and protein; and
4 the change of the entropy accompanying the P−L complex formation in a water environment.

All of the contributions are important, and none of them can be neglected. Most attention is paid to the evaluation of the first two energies, and in the majority of cases the empirical potentials or even their simplifications are used.[8,10,11] Their main drawback consists of their neglecting the quantum effects (proton and electron transfer, description of the halogen bond etc.), which is, however, correctly covered by our SQM PM6-DH2 method. Another important feature of our new score is that every physical term is calculated using the most accurate method available. The score is thus constructed as a sum of the PM6-DH2 interaction enthalpy,[12,13] changes in the SMD solvation and PM6-DH2 deformation energies[14] and the empirical-force-field-based vibrational entropy change. No adjustable empirical

Received: January 31, 2011
Revised: March 22, 2011
Published: April 05, 2011

ACS Publications © 2011 American Chemical Society

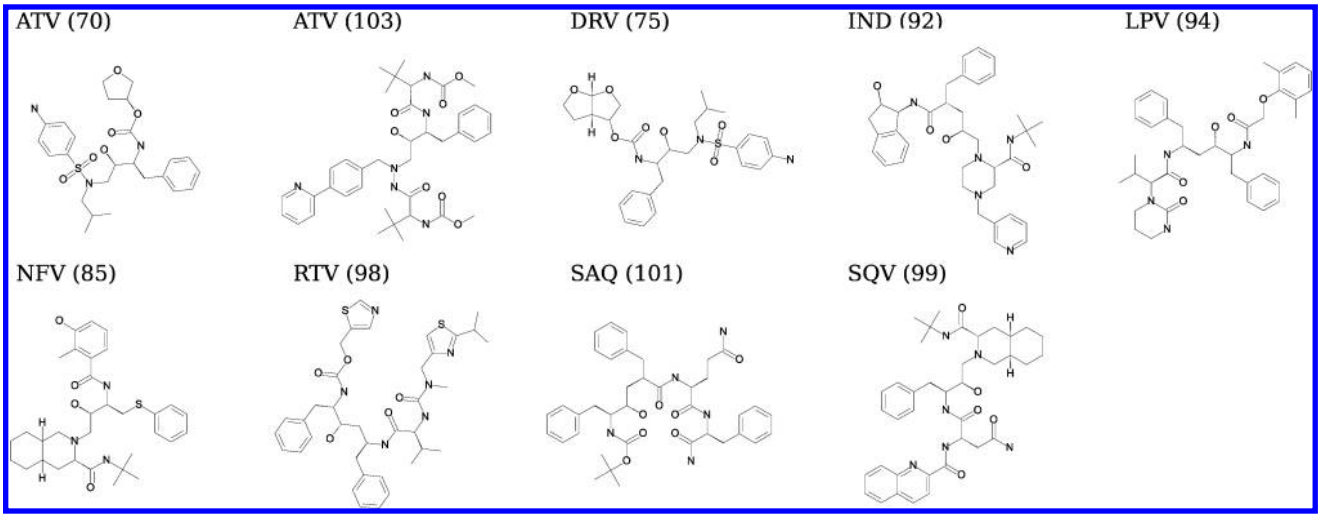

Figure 1. The chemical formulas of the HIV-1 PR inhibitors with their abbreviations. The number of atoms is provided in the parentheses.

parameters for the particular energetic terms and for specific ligands are used as was the case, for instance, in references 15−17.

This scoring approach was successfully applied on two series of diverse inhibitors, namely, HIV-1 protease (PR)[9] and CDK2 kinase inhibitors.[18] In both studies, the interaction enthalpies of the P−L complexes represent the dominant terms, and, owing to the reliable PM6-DH2 technique, we expect these to be sufficiently accurate. (For the twenty-two complexes included in the S22 data set, the PM6-DH2 method provides interaction energies within 1 kcal·mol^{-1} of the benchmark CCSD(T) values.)[13]

In the case of evaluation of the solvation/desolvation free energies, the situation is, however, different. In both studies mentioned above, the desolvation energies of the ligands were very large, comparable to the interaction enthalpies, but with the opposite sign. While the interaction enthalpies are negative and thus encourage binding, the ligand desolvation free energies are positive and thus oppose the binding. The main problem here, however, originates not in the choice of the solvation model but in the choice of the ligand structure used for the evaluation of the change of the solvation free energy.

The solvation free energy is quite well-defined for rigid molecules such as benzene or methane. It represents the free energy change connected with the transfer of the molecule from the gas phase (vacuum) into bulk water. For a flexible molecule, the interpretation of the solvation free energy is not straightforward. In this case, we cope with an ensemble of distinct conformations, and the solvation energy calculated for a single conformation stands for the free energy of the vacuum−water transfer under the assumption that the single conformation represents an equilibrium structure of the molecule in both the vacuum and solvated states. It is, however, not very clear to what extent this assumption is valid.

Our score contains a term which describes a change of the solvation free energy upon ligand binding. Apart from the protein solvation energy change, this is constructed as the difference of the solvation energy of a ligand conformation in water and of the ligand conformation restrained by protein surroundings. The conformation in a water environment is often approximated by a structure taken from the P−L complex that is optimized with an implicit solvent.[9,17] More reliable ligand conformations are expected from the molecular dynamics (MD) simulations followed by a gradient optimization (quenching technique). In the case of rigid ligands, the optimization with an implicit solvent model is justified. However, for a flexible ligand, the latter approximation seems to be better suited.

In the present paper, we have reexamined the choice of the ligand conformation for which the solvation energy is computed by performing a standard MD simulation and by calculating the conformational energy. We selected complexes of HIV-1 protease with nine inhibitors which had been briefly studied in our previous paper. All of the inhibitors considered are very flexible. Here, the conformational energy denotes the sum of the solvation energy calculated for a particular ligand conformation and of the gas phase electronic energy which also relates to the particular ligand conformation. The difference of the electronic energies between the two different conformations would be called "deformation energy" and the difference of the solvation energies between the two conformations would be called the "change in solvation energy". When considering the P−L binding, one of the two conformations represents a bonded state in a protein environment and the other represents the free state in water.

The molecular dynamics simulations of the nonstandard residues with an empirical potential usually face a problem of partial charges. In MD, the concept of the point charges is claimed to be essential even though the results might depend on the choice of the atomic partial charges. Several publications have tackled this issue.[19−21] Throughout the study, the General Amber Force Field (GAFF)[22] was employed. The designers of the force field recommend partial charges evaluated on the bases of the RESP technique[23] or calculated at the AM1-BCC level of theory.[24,25] We chose the RESP charges since the AM1-BCC are parametrized to reproduce the RESP charges, as a result of which the RESP charges should be more reliable. However, the charges of both methods might be conformationally dependent, and it can be expected that this dependence increases with the increasing number of possible conformers. To eliminate any possible dependency, we sampled the conformations with ten different charge sets.

2. METHODS

We have studied the conformational energies of nine HIV-1 protease inhibitors, namely, amprenavir (APV) 1HPV,[26] atazanavir (ATV) 2AQU,[27] darunavir (DRV) 1T3R,[28] indinavir (IDV) 2BPX,[29] lopinavir (LPV) 1MUI,[30] nelfinavir (NFV) 1OHR,[31] ritonavir (RTV) 1HXW,[32] Boc-Phe-Psi[(S)-CH(OH)CH2NH]-Phe-Gln-Phe-NH2 (SAQ) 1IIQ[33] and saquinavir (SQV) 3CYX.[34] All nine ligands (see Figure 1) were considered to be neutral, which is consistent with our previous work.[9] The biological activities of the ligands are presented in references 35−39.

The estimations of the conformational energies of nine HIV PR inhibitors were performed in several steps: presampling, sampling, and energy estimation. We plotted the probability density functions of the energies and calculated their mean values. The probability density function describes how likely is to find the conformation with such an energy. Since called "probability", it is normalized to yield 1 when integrated.

The probability density functions of the energies were compared with the results obtained from a short MD simulation with a PM6-DH2 potential and with a single value calculated with the ligand conformation presented in the P−L complex optimized with an implicit solvent. In that sense, the mean values of the probability density functions are considered as the "correct" ones (i.e., not suffering from the single-conformation approximation) and the comparison of the values obtained by other protocols is presented with respect to them.

2.1. Presampling. The P−L complex's experimental geometry was optimized at the PM6-DH2 level. The grid of the electrostatic potential (ESP) points was calculated around the bare ligand structure on the HF/6-31G* level.[40,41] The partial charges were fitted onto the grid according to the RESP methodology; typically about 8000 grid points were used for the fit. The bond, angle, torsion and atomic Lennard-Jones parameters of each of the nine HIV PR inhibitors were assigned from the GAFF force field using the Antechamber program from the Amber program package[42] with the default setup.

Each ligand was surrounded by TIP3P water molecules[43] in a cubic periodic box. The distance of the ligand from the edge of the box was 1 nm, which resulted in approximately 1500 water molecules in the box. A short minimization of the ligand and water molecules was performed to avoid any possible close contacts. The system was heated during a 50 ps simulation with the box volume kept constant, which was followed by a 200 ps equilibration at a temperature of 300 K and under a pressure of 1 bar. A Berendsen thermostat and barostat were employed.[44] The production consisted of a 200 ps simulation at a temperature of 700 K and under a pressure of 1 bar. The time step of 1 fs was used, and the structure of the ligand was saved every 20 ps.

For each ligand, this yielded ten structures. Owing to the high temperature, a variety of conformations was visited during rather short MD simulations. It may be a question if the GAFF force field, originally proposed for simulations at 300 K, is well-behaved for simulations at significantly elevated temperature. However, the conformations obtained at 700 K need not represent the dynamics accurately here, since they only serve as the initial points for the sampling, which was indeed done at 300 K. The variability of the ten conformations is demonstrated by a root-mean-square deviation from the starting structure, which was typically 0.35 nm.

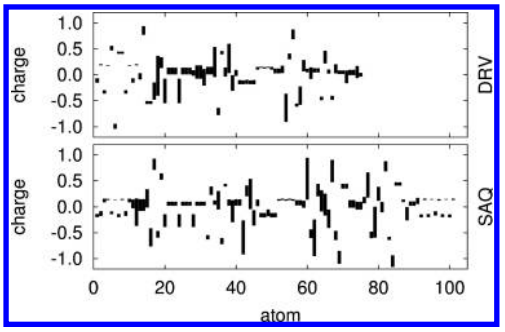

Figure 2. The variations of the atomic partial charges. For each atom, the range between the minimum and maximum charge within the ten charge sets is plotted. The ligand with the most negative binding free energy (DRV) and the ligand with the least negative binding free energy (SAQ)[35−39] were chosen for illustration. The complete set of ligands is available in the Supporting Information.

2.2. Sampling. For each ligand, ten conformations were used for a reevaluation of the RESP charges. Each ligand structure was optimized at the PM6-DH2 level with the COSMO implicit solvation model,[45] the HF/6-31G* ESP points were calculated and the partial charges were fitted onto them. The other parameters were taken from the GAFF force field as mentioned above.

The water box preparation and equilibration protocol was the same as described in the presampling section. Hereafter, ten 40 ns MD simulations of ligands with different RESP charge sets were performed for each ligand at a temperature of 300 K and under a pressure of 1 bar. A Nosé−Hoover thermostat[46,47] and Parrinello−Rahmann barostat[48] were used to obtain the correct isobaric−isothermal ensemble. The ligand structures were saved every 250 ps, which yielded 160 structures for each charge set. For all of the MD simulations, the Gromacs program package was used.[49]

2.3. SMD and Gas Phase Energies. Each structure was optimized at the PM6-DH2 level with the COSMO implicit solvation model until the convergence criteria (the energy difference between the two consecutive steps lower than 6×10^{-3} kcal·mol^{-1} and a maximal gradient lower than 1.2 kcal·mol^{-1}·A^{-1}) were satisfied. With the final structure, the gas-phase PM6-DH2 energy (denoted E_{vac}) and solvation SMD/HF/6-31G* energy (denoted E_{SMD}) were calculated. The sum of the two respective energies is presented as the conformational energy (denoted E_{conf}). In total, 1600 conformations for each of the nine HIV PR inhibitors were evaluated. The normalized probability density functions of the solvation, gas-phase electronic and conformational energies were calculated.

2.4. PM6-DH2 Optimization and Quenching. The ligand coordinates were taken from the PM6-DH2 optimized P−L complex and reoptimized with the implicit COSMO model at the PM6-DH2 level. The solvation SMD, gas-phase PM6-DH2 and conformational energies—the sum of the previous two—were calculated on the final structure. These values are referred to as the "PM6-DH2 optimization" energies.

The PM6-DH2 simulations were performed with the implicit COSMO water model. A temperature of 500 K was kept constant by an Andersen thermostat.[50] The total simulation time was 50 ps with a time step of 1 fs. The ligand coordinates were saved every picosecond, after which they were optimized at the PM6-DH2 level with the COSMO water model. On the final

Table 1. The Standard Deviations (std) of the Mean Values of the Probability Density Functions[a]

ligand	APV	ATV	DRV	IND	LPV	NFV	RTV	SAQ	SQV
std(E_{SMD})	0.76	0.44	0.79	1.16	0.53	0.58	0.59	0.82	2.03
std(E_{vac})	2.03	0.45	1.29	3.98	1.02	0.89	0.69	0.81	3.00
std(E_{conf})	1.37	0.44	0.55	3.57	0.87	1.10	0.54	0.63	1.74

[a] E_{SMD} stands for SMD solvation energy, E_{vac} stands for gas-phase PM6-DH2 energy, and E_{conf} stands for conformational energy, the sum of the previous two. The standard deviations are calculated for the set of ten mean values obtained from ten 40 ns long simulations. The simulations differ in the charge set describing the ligand and the initial conformation of the MD. All of the values are in kcal·mol^{-1}.

structures, the E_{SMD}, E_{vac} and E_{conf} were calculated and are referred to as the "PM6-DH2 quench" energies. All of the PM6-DH2 optimizations were performed with the same convergence criteria (mentioned above).

For the PM6-DH2 and SMD calculations, Gaussian09[51] and Mopac[52] programs were used.

3. RESULTS AND DISCUSSIONS

3.1. MD Simulations. For each ligand, we performed a series of MD simulations which differed in the set of atomic partial charges. The charges were calculated for ten different conformations (see Methods). Figure 2 shows the range of the charges for two ligands. The difference between the minimal and maximal charge within the set is plotted for each atom. About 10% of the atoms usually embody a large conformational dependence while the rest remain quite independent. The largest variation reaches 0.802 e for a carbon atom in one of the SAQ carbonyl groups. This extremely large variation is, however, not accompanied by a comparably large change in the conformational energy (see below). We expect the lower variations of the charges of the other atoms to compensate for the rarely occurrences of large variations. It is surprising that the conformational energy is not very sensitive to the particular charge distribution. Part of the conformational energy insensitivity might also be "hidden" in the subsequent geometry optimization, which is always done at the semiempirical PM6-DH2 level with a relatively correct charge distribution and which might buffer the inaccuracy of the RESP charge models.

All of the simulations were stable; the fluctuations in temperature and pressure were within the normal range. In total, 400 ns for each ligand were simulated. We believe that the simulations sufficiently converge with respect to the mean values of particular energies. The mean values of the 40 ns long simulations differ only slightly. Their standard deviations are summarized in Table 1. The entire probability density functions of darunavir (DRV) are shown in Figure 3; the probability density functions of all of the ligands are available in the Supporting Information.

The standard deviations from Table 1 might serve as a measure of two characteristics: first, the convergence of the simulations, and second, the conformational dependence of the RESP charges. The fact that some atomic partial charges vary significantly seems to be quite unimportant in the sense of the SMD solvation energy as well as the vacuum PM6-DH2 energy. The probability density functions of all of the ten simulations (Figure 3, DRV) are normal-like and localized with very similar mean values. One has to bear in mind that there were ten different starting conformations differing in partial charges on the atoms. In the case of DRV, the RMSDs of the heavy atoms with respect to the conformation 0 were within the range of 0.171 to 0.384 nm.

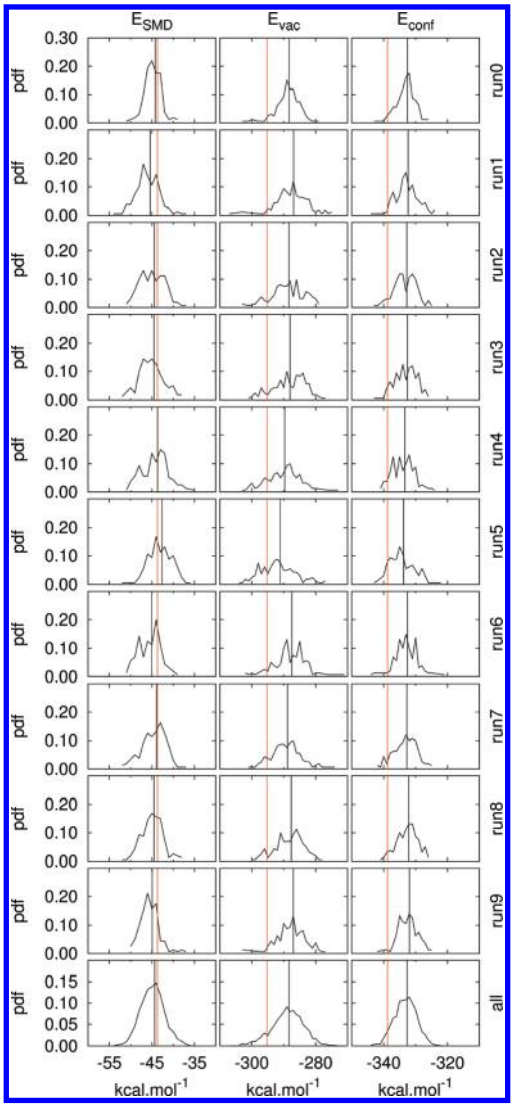

Figure 3. The probability density functions (pdf) of the SMD solvation energy (E_{SMD}), gas-phase PM6-DH2 energy (E_{vac}) and their sum, conformational energy (E_{conf}). The pdfs for the different charge sets calculated for ten ligand conformations are plotted. The pdfs are constructed from the set of 160 values of each particular energy. The 1600 values of all of the runs were used for the last row ("all"). The black vertical line indicates the mean value of pdf; the orange lines indicate the values from the PM6-DH2 quench. The plots describing the most potent drug, darunavir (DRV), were chosen for illustration. All of the ligands are available in the Supporting Information.

3.2. Energies. The probability density functions are plotted in Figure 4. They were calculated for the set of 1600 values obtained by the extensive MD sampling with an empirical potential (see Methods). This does not, however, mean that the energies are based on an empirical potential. The minimization at the PM6-DH2 level ensures the relaxation of the snapshot from the empirical MD onto a semiempirical potential energy surface (PES). The conformation then represents the nearest semiempirical minimum of the empirical PES.

The mean values of the probability density functions in Figure 4 are also summarized in Tables 2 and 3 together with

dx.doi.org/10.1021/jp2010265 |J. Phys. Chem. B 2011, 115, 4718–4724

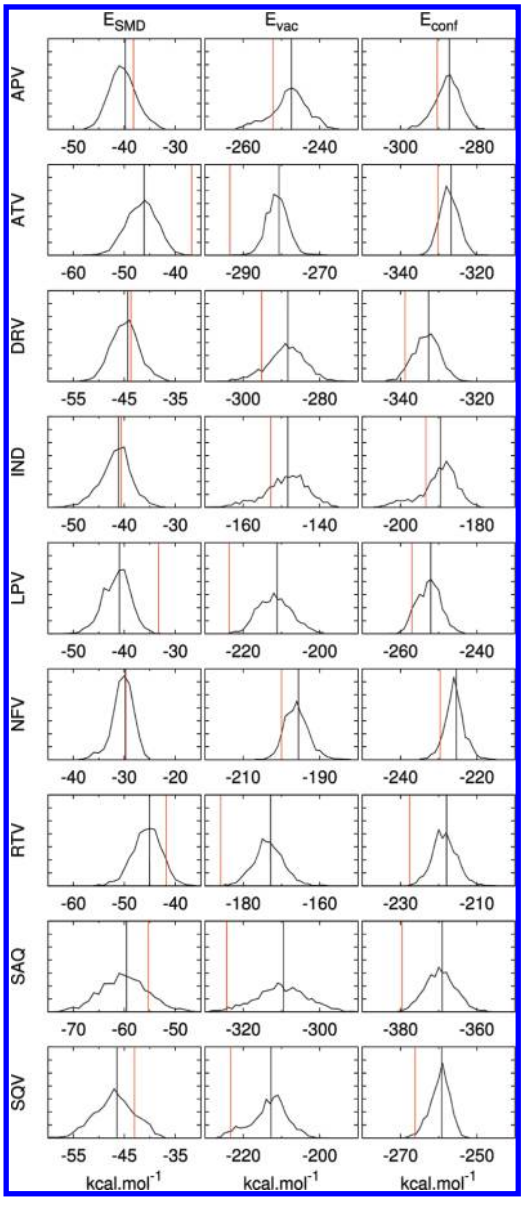

Figure 4. The probability density functions (pdfs) of the SMD energy (E_{SMD}), the gas-phase PM6-DH2 energy (E_{vac}) and their sum (E_{conf}). The pdfs are calculated for each ligand from the set of 1600 conformations obtained from the ten MD simulations with the various charge sets. Note the same range of *x*-axes (in kcal·mol^{-1}). The black vertical lines indicate the mean value of pdf; the orange lines indicate the values from the PM6-DH2 quench.

the PM6-DH2 quench and PM6-DH2 optimization values, respectively. In Figure 4, the mean values are plotted as vertical black lines, whereas the orange lines represent the values from the PM6-DH2 quench. For each ligand and each energy, we calculated the mean value and the standard deviation over the set of ten simulations.

Omitting the flexibility of the ligand, i.e. considering those values not obtained from extensive conformation sampling, we introduce an error. Here, we present the errors connected genuinely with the single-conformation approximation of various extents (PM6-DH2 optimization and PM6-DH2 quench) when compared with MD sampling, which is indeed multiple-conformation approach.

Table 2. The Distinctions between the Extensive MD Sampling and the PM6-DH2 Optimization[a]

ligand	APV	ATV	DRV	IND	LPV	NFV	RTV	SAQ	SQV	avg	std
ΔE_{SMD}	3.6	1.9	3.1	−4.9	3.9	−6.9	2.3	2.2	−1.3	0.4	3.9
ΔE_{vac}	0.8	−0.7	−1.7	11.3	−1.3	2.9	−4.3	2.9	−0.1	1.1	4.5
ΔE_{conf}	4.4	1.3	1.4	6.5	2.6	−4.0	−2.0	5.1	−1.3	1.5	3.5

[a] The differences E(optim) − E(MD) are shown in kcal·mol^{-1}. The averages (avg) and standard deviations (std) are calculated over the set of ligands. ΔE_{SMD} stands for the difference of the SMD solvation energies, ΔE_{vac} of the gas-phase PM6-DH2 energies and ΔE_{conf} of the conformational energies. The absolute values of the energies are provided in the Supporting Information.

Table 3. The Distinctions between the Extensive MD Sampling and the Short PM6-DH2 Quench[a]

ligand	APV	ATV	DRV	IND	LPV	NFV	RTV	SAQ	SQV	avg	std
ΔE_{SMD}	1.6	9.3	0.7	0.5	7.6	0.2	3.3	4.2	3.5	3.4	3.2
ΔE_{vac}	−4.8	−12.8	−6.8	−4.5	−12.5	−4.4	−13.0	−14.8	−10.6	−9.4	4.2
ΔE_{conf}	−3.2	−3.5	−6.2	−4.0	−4.9	−4.3	−9.7	−10.6	−7.1	−5.9	2.7

[a] The difference of E(quench) − E(MD) is shown in kcal·mol^{-1}. The averages (avg) and standard deviations (std) are calculated over the set of ligands. ΔE_{SMD} stands for the difference of the SMD solvation energies, ΔE_{vac} of the PM6-DH2 gas-phase energies and ΔE_{conf} of the conformational energies. The absolute values of the energies are provided in the Supporting Information.

For the set of nine HIV PR inhibitors, the average error in the SMD solvation energy of the PM6-DH2 optimization (see Table 2) is 0.4 kcal·mol^{-1} with a standard deviation of 3.9 kcal·mol^{-1}. The average of E_{vac} is 1.1 kcal·mol^{-1} with a standard deviation of 4.5 kcal·mol^{-1}. The sum of ΔE_{SMD} and ΔE_{vac} increases the average to 1.5 kcal·mol^{-1} while it decreases the standard deviation to 3.5 kcal·mol^{-1}.

The aim of the scoring is to rank the ligands according to their binding free energy or, in other words, on the bases of the score to distinguish the effective binders from the weak binders or nonbinders. In that sense, the average values of the errors (i.e., absolute errors) are rather unimportant, because they represent an average shift of all of the ligands. For a correct ranking, one tries to minimize the relative shift between the ligands, as a consequence of which the standard deviations (relative errors), which tell us with what uncertainty the ligands might be sorted, deserve greater attention.

The PM6-DH2 optimization yields structures which are similar to those in the P−L complex. This results in a quite small absolute error with a significant relative error. What seems to be important is the fact that the differences between the MD sampling and PM6-DH2 optimization are not of the same "sign". Undesirably, the ΔE_{conf} is negative for NFV, RTV and SQV, whereas it is positive for the rest of the ligands. That fact is reflected in the standard deviation of ΔE_{conf} being 3.5 kcal·mol^{-1}.

Table 3 and Figure 4 show that even a short PM6-DH2 quench (MD followed by geometry optimization, see Methods) can improve the results reasonably. In the case of ΔE_{SMD}, the error is systematically shifted (cf. Figure 3) for all of the ligands. When comparing the ΔE_{SMD} energies from the MD sampling and the PM6-DH2 quench, the former are more negative by an average value of 3.4 kcal·mol^{-1}, with the standard deviation being 3.5 kcal·mol^{-1}. The E_{vac} are shifted in the opposite direction by an

average value of -9.4 kcal·mol^{-1}, with a standard deviation of 4.2 kcal·mol^{-1}. These shifts are partially compensated for, which results in an average ΔE_{conf} of -5.9 kcal·mol^{-1}, with the standard deviation being 2.7 kcal·mol^{-1}.

The range of the scores for the series of HIV PR binders was about 50 kcal·mol^{-1} (from -15 to $+35$ kcal·mol^{-1}).[9] A similar difference in the score between the strong and weak binders was also obtained for the CDK2 ligands.[18] Hence, the uncertainty arising from the choice of ligand conformation representing the equilibrium conformation in a water environment is 2.7 kcal·mol^{-1}, which is about 5% of the range of the total scores calculated. The implication of this uncertainty for our scoring is that if the score differs by less than about 2.7 kcal·mol^{-1}, the only conclusion is that such ligands are predicted to have similar binding activity. This limitation seems to be in most cases minor. It should be noted that HIV PR ligands are of a peptidomimetic character (a protein-like chain that mimics a peptide) and are thus extremely flexible, which is also evident in the probability density functions (Figure 4). The variation might be smaller when more rigid molecules are scored.

Even though the HIV PR inhibitors exhibit quite large conformational flexibility, none of the studied ligands shows a multiple-maxima probability density function of energy. This indicates that it is possible to choose a single conformation which would represent the ligand conformational energy of the equilibrium ensemble in an aqueous environment. Nevertheless, we admit that the choice of the proper conformation might not be straightforward and should be the object of further studies.

4. CONCLUSIONS

We estimated the uncertainty with which the conformational energy is calculated in our scoring function based on the quantum mechanical PM6-DH2 method. From extensive MD sampling at 300 K, we calculated the average values and standard deviations of the SMD solvation energy, gas-phase PM6-DH2 energy and their sum—the conformational energy—of nine HIV PR inhibitors. These energies were compared with the energies obtained by two other approaches.

The simplest approach (PM6-DH2 optimization) provides a relative uncertainty of about 3.5 kcal·mol^{-1} while the more demanding PM6-DH2 quenching improves this to 2.7 kcal·mol^{-1}. The extent of the flexibility of the inhibitors was demonstrated by the probability density functions of energy, based on 400 ns of simulations in total. From the simulations, the choice of the conformation which is used for the calculation of the atomic partial charges appears to be rather unimportant with respect to the conformational energy.

In the scoring studies based on rigid molecules (i.e., single-conformation approach), our results indicate an error brought by the approximation of neglect of flexibility. The results suggest that the resolution with which the scores can be interpreted is limited. The difference within the range of single kilocalories in the score might be misleading. However, this uncertainty is considerably smaller than the discrimination between binders and nonbinders, or between strong and weak binders. The uncertainty presented in this study then represents only a few percent of the score difference between those groups of ligands.

■ ASSOCIATED CONTENT

Ⓢ Supporting Information. The values of the E_{SMD}, E_{vac} and E_{conf} of all of the ligands, the plots of the charge variations for all of the ligands and the probability density functions of E_{SMD}, E_{vac} and E_{conf} for all of the ligands. This material is available free of charge via the Internet at http://pubs.acs.org.

■ AUTHOR INFORMATION

Corresponding Author

*E-mail: pavel.hobza@uochb.cas.cz.

■ ACKNOWLEDGMENT

This work was supported by the Institute of Organic Chemistry and Biochemistry, Academy of Sciences of the Czech Republic [Z40550506], the Ministry of Education, Youth and Sports of the Czech Republic [LC512 and MSM6198959216], the Czech Science Foundation [P208/11/0295] and Korea Science and Engineering Foundation [World Class Univ. program: R32-2008-000-10180-0]. This work was also supported by the Operational Program Research and Development for Innovations—European Science Fund (CZ.1.05/2.1.00/03.0058). The support of Praemium Academiae, Academy of Sciences of the Czech Republic, awarded to P.H. in 2007 is also acknowledged.

■ REFERENCES

(1) Raha, K.; Merz, K. M., Jr. *J. Med. Chem.* **2005**, *48*, 4558–4575.
(2) Friesner, R. A.; Murphy, R. B.; Repasky, M. P.; Frye, L. L.; Greenwood, J. R.; Halgren, T. A.; Sanschagrin, P. C.; Mainz, D. T. *J. Med. Chem.* **2006**, *49*, 6177–6196.
(3) Kirkwood, J. G. *J. Chem. Phys.* **1935**, *3*, 300–313.
(4) Chipot, C.; Pohorille, A. *Free Energy Calculations*, Springer-Verlag: Berlin, 2007.
(5) Zwanzig, R. W. *J. Chem. Phys.* **1954**, *22*, 1420–1426.
(6) Huang, D.; Caflisch, A. *J. Mol. Recognit.* **2009**, *23*, 183–193.
(7) Zhou, T.; Caflish, A. *Chem. Med. Chem.* **2010**, *5*, 1007–1014.
(8) Sousa, S. F.; Fernandes, P. A.; Ramos, M. J. *Proteins: Struct., Funct., Bioinf.* **2006**, *65*, 15–26.
(9) Fanfrlík, J.; Bronowska, A. K.; Řezáč, J.; Přenosil, O.; Konvalinka, J.; Hobza, P. *J. Phys. Chem. B* **2010**, *114*, 12666–12678.
(10) DeWitte, R. S.; Shakhnovich, E. I. *J. Am. Chem. Soc.* **1996**, *118*, 11733–11744.
(11) Essex, J. *J. Comput.-Aided Mol. Des.* **2002**, *16*, 151–166.
(12) Řezáč, J.; Fanfrlík, J.; Salahub, D.; Hobza, P. *J. Chem. Theory Comput.* **2009**, *5*, 1749–1760.
(13) Korth, M.; Pitoňák, M.; Řezáč, J.; Hobza, P. *J. Chem. Theory Comput.* **2010**, *6*, 344–352.
(14) Marenich, A. V.; Cramer, C. J.; Truhlar, D. G. *J. Phys. Chem. B* **2009**, *113*, 6378–96.
(15) Friedman, R.; Caflisch, A. *Chem. Med. Chem.* **2009**, *4*, 1317–1326.
(16) Huang, D.; Caflisch, A. *J. Mol Recognit.* **2009**, *23* (2), 183–193.
(17) Hayik, S. A.; Dunbrack, R.; Merz, K. M. *J. Chem. Theory Comput.* **2010**, *6*, 3079–3091.
(18) Dobeš, P.; Fanfrlík, J.; Řezáč, J.; Otyepka, M.; Hobza, P. *J. Comput.-Aided Mol. Des.* **2011**, *25*, 223–235.
(19) Okamoto., Y.; Tanaka, T.; Kokubo, H. *J. Comput.-Aided Mol. Des.* **2010**, *24*, 699–712.
(20) Söderhjelm, P.; Ryde, U. *J. Comput. Chem.* **2009**, *30*, 750–760.
(21) Shivakumar, D.; Deng, Y. Q.; Roux, B. *J. Chem. Theory Comput.* **2009**, *5*, 919–930.
(22) Wang, J.; Wolf, R. M.; Caldwell, J. W.; Kollman, P. A.; Case, D. A. *J. Comput. Chem.* **2004**, *25*, 1157–1174.
(23) Bayly, C. I.; Cieplak, P.; Cornell, W.; Kollman, P. A. *J. Phys. Chem.* **1993**, *97*, 10269–10280.

(24) Jakalian, A.; Bush, B. L.; Jack, D. B.; Bayly, C. I. *J. Comput. Chem.* **2000**, *21*, 132–146.
(25) Jakalian, A.; Jack, D. B.; Bayly, C. I. *J. Comput. Chem.* **2002**, *23*, 1623–1641.
(26) Kim, E. E.; Baker, C. T.; Dwyer, M. D.; Murcko, M. A.; Rao, B. G.; Tung, R. D.; Navia, M. A. *J. Am. Chem. Soc.* **1995**, *117*, 1181–1182.
(27) Clemente, J. C.; Coman, R. M.; Thiaville, M. M.; Janka, L. K.; Jeung, J. A.; Nukoolkarn, S.; Govindasamy, L.; Agbandje-McKenna, M.; McKenna, R.; Leelamanit, W.; Goodenow, M. M.; Dunn, B. M. *Biochemistry* **2006**, *45*, 5468–5477.
(28) Surleraux, D. L. N. G.; Tahri, A.; Verschueren, W. G.; Pille, G. M. E.; de Kock, H. A.; Jonckers, T. H. M.; Peeters, A.; De Meyer, S.; Azijn, H.; Pauwels, R.; de Bethune, M. P.; King, N. M.; Prabu-Jeyabalan, M.; Schiffer, C. A.; Wigerinck, P. B. T. P. *J. Med. Chem.* **2005**, *48*, 1813–1822.
(29) AMunshi, S.; Chen, Z.; Li, Y.; Olsen, D. B.; Fraley, M. E.; Hungate, R. W.; Kuo, L. C. *Acta Crystallogr., Sect. D* **1998**, *54*, 1053–1060.
(30) Stoll, V.; Qin, W.; Stewart, K. D.; Jakob, C.; Park, C.; Walter, K.; Simmer, R. L.; Helfrich, R.; Bussiere, D.; Kao, J.; Kempf, D.; Sham, H. L.; Norbeck, D. W. *Bioorg. Med. Chem.* **2002**, *10*, 2803–2806.
(31) Kaldor, S. W.; Kalish, V. J.; Davies, J. F., II; Shetty, B. V.; Fritz, J. E.; Appelt, K.; Burgess, J. A.; Campanale, K. M.; Chirgadze, N. Y.; Clawson, D. K.; Dressman, B. A.; Hatch, S. D.; Khalil, D. A.; Kosa, M. B.; Lubbehusen, P. P.; Muesing, M. A.; Patick, A. K.; Reich, S. H.; Su, K. S.; Tatlock, J. H. *J. Med. Chem.* **1997**, *40*, 3979–3985.
(32) Kempf, D. J.; Marsh, K. C.; Denissen, J. F.; McDonald, E.; Vasavanonda, S.; Flentge, C. A.; Green, B. E.; Fino, L.; Park, C. H.; Kong, X. P. *Proc. Natl. Acad. Sci. U.S.A.* **1995**, *92*, 2484–2488.
(33) Dohnálek, J.; Hašek, J.; Dušková, J.; Petroková, H.; Hradílek, M.; Souček, M.; Konvalinka, J.; Brynda, J.; Sedláček, J.; Fabry, M. *J. Med. Chem.* **2002**, *45*, 1432–1438.
(34) Liu, F. L.; Kovalevsky, A. Y.; Tie, Y.; Ghosh, A. K.; Harrison, R. W.; Weber, I. T. *J. Mol. Biol.* **2008**, *381*, 102–115.
(35) Petroková, H.; Dušková, J.; Dohnálek, J.; Skálová, T.; Vondráčková-Buchtelová, E.; Souček, M.; Konvalinka, J.; Brynda, J.; Fábry, M.; Sedláček, J.; Hašek, J. *Eur. J. Biochem.* **2004**, *271*, 4451–61.
(36) Urban, J.; Konvalinka, J.; Stehlíková, J.; Gregorová, E.; Majer, P.; Souček, M.; Andreánský, M.; Fábry, M.; Strop, P. *FEBS Lett.* **1992**, *298*, 9–13.
(37) Majer, P.; Urban, J.; Gregorová, E.; Konvalinka, J.; Novek, P.; Stehlíková, J.; Andreánský, M.; Sedláček, J.; Strop, P. *Arch. Biochem. Biophys.* **1993**, *304*, 1–8.
(38) Konvalinka, J.; Litera, J.; Weber, J.; Vondrášek, J.; Hradílek, M.; Souček, M.; Pichová, I.; Majer, P.; Strop, P.; Sedláček, J.; Heuser, A. M. *Eur. J. Biochem.* **1997**, *250*, 559–566.
(39) Kottler, H.; Kräusslich, H. G. *Eur. J. Biochem.* **1997**, *250*, 559–566.
(40) Roothaan, C. C. J. *Rev. Mod. Phys.* **1951**, *23*, 69–89.
(41) Hariharan, P. C.; Pople, J. A. *Theor. Chem. Acc.* **1973**, *28*, 213–22.
(42) Case, D. A.; Darden, T. A.; Cheatham, T. E., III; Simmerling, C. L.; Wang, J.; Duke, R. E.; Luo, R.; Crowley, M.; Walker, R. C.; Zhang, W.; Merz,K. M.; Wang, B.; Hayik, S.; Roitberg, A.; Seabra, G.; Kolossváry, I.; Wong, K. F.; Paesani, F.; Vanicek, J.; Wu, X.; Brozell, S. R.; Steinbrecher, T.; Gohlke, H.; Yang, L.; Tan, C.; Mongan, J.; Hornak, V.; Cui, G.; Mathews, D. H.; Seetin, M. G.; Sagui, C.; Babin, V.; Kollman, P. A. *AMBER 10*; University of California: San Francisco, 2008.
(43) Jorgensen, W. L. *J. Am. Chem. Soc.* **1981**, *103*, 335–340.
(44) Berendsen, H. J. C.; Postma, J. P. M.; van Gunsteren, W. F.; Dinola, A.; Haak, J. R. *J. Chem. Phys.* **1984**, *81*, 3684–3690.
(45) Klamt, A.; Schuurmann, G. *J. Chem. Soc., Perkin Trans.* **1993**, *2*, 799–805.
(46) Nosé, S. *Mol. Phys.* **1984**, *52*, 255–268.
(47) Hoover, W. G. *Phys. Rev. A* **1985**, *31*, 1695–1697.
(48) Parrinello, M.; Rahman, A. *J. App. Phys.* **1981**, *52*, 7182–7190.
(49) Hess, B.; Kutzner, C.; van der Spoel, D.; Lindahl, E. *J. Chem. Theory Comput.* **2008**, *4*, 435–447.
(50) Andersen, H. C. *J. Chem. Phys.* **1980**, *72*, 2384–2393.
(51) Frisch, M. J.; Trucks, G. W.; Schlegel, H. B.; Scuseria, G. E.; Robb, M. A.; Cheeseman, J. R.; Scalmani, G.; Barone, V.; Mennucci, B.; Petersson, G. A.; Nakatsuji, H.; Caricato, M.; Li, X.; Hratchian, H. P.; Izmaylov, A. F.; Bloino, J.; Zheng, G.; Sonnenberg, J. L.; Hada, M.; Ehara, M.; Toyota, K.; Fukuda, R.; Hasegawa, J.; Ishida, M.; Nakajima, T.; Honda, Y.; Kitao, O.; Nakai, H.; Vreven, T.; Montgomery, J. A., Jr.; Peralta, J. E.; Ogliaro, F.; Bearpark, M.; Heyd, J. J.; Brothers, E.; Kudin, K. N.; Staroverov, V. N.; Kobayashi, R.; Normand, J.; Raghavachari, K.; Rendell, A.; Burant, J. C.; Iyengar, S. S.; Tomasi, J.; Cossi, M.; Rega, N.; Millam, N. J.; Klene, M.; Knox, J. E.; Cross, J. B.; Bakken, V.; Adamo, C.; Jaramillo, J.; Gomperts, R.; Stratmann, R. E.; Yazyev, O.; Austin, A. J.; Cammi, R.; Pomelli, C.; Ochterski, J. W.; Martin, R. L.; Morokuma, K.; Zakrzewski, V. G.; Voth, G. A.; Salvador, P.; Dannenberg, J. J.; Dapprich, S.; Daniels, A. D.; Farkas, O.; Foresman, J. B.; Ortiz, J. V.; Cioslowski, J.; Fox, D. J. *Gaussian 09*, Revision A.1; Gaussian, Inc.: Wallingford, CT, 2009.
(52) Stewart, J. J. P. *Stewart Computational Chemistry*, Colorado Springs, CO, MOPAC2009; http://OpenMOPAC.net.